

AB598, a Therapeutic Anti-CD39 Antibody, Elevates ATP and Increases Immunogenicity in the Tumor Microenvironment



Kaustubh Parashar, Julie Clor, Dana Piovesan, Casey Mitchell, LC Stetson, Ke Jin, Gonzalo Barajas, Sean Cho, Janine Kline, Stephen W. Young, Nigel P. Walker, Matthew J. Walters, Ester Fernandez-Salas, Christine E. Bowman

Arcus Biosciences, Inc.; 3928 Point Eden Way, Hayward, CA 94545 (USA)

INTRODUCTION

❖ AB598, an IgG1 Fc-silent antibody that blocks CD39 (*ENTPD1*) enzymatic activity, is being developed as a novel cancer immunotherapy. CD39 is highly expressed on immune and stromal cells within the tumor microenvironment (TME) and is responsible for the conversion of adenosine triphosphate (ATP) into adenosine monophosphate (AMP).

❖ **Therapeutic Hypothesis:** AB598 can bind and inhibit CD39 activity on immune cells, leading to an increase in local levels of immunostimulatory ATP. In the TME, elevated ATP exerts its effects by signaling through members of the P2X and P2Y purinergic receptor families.

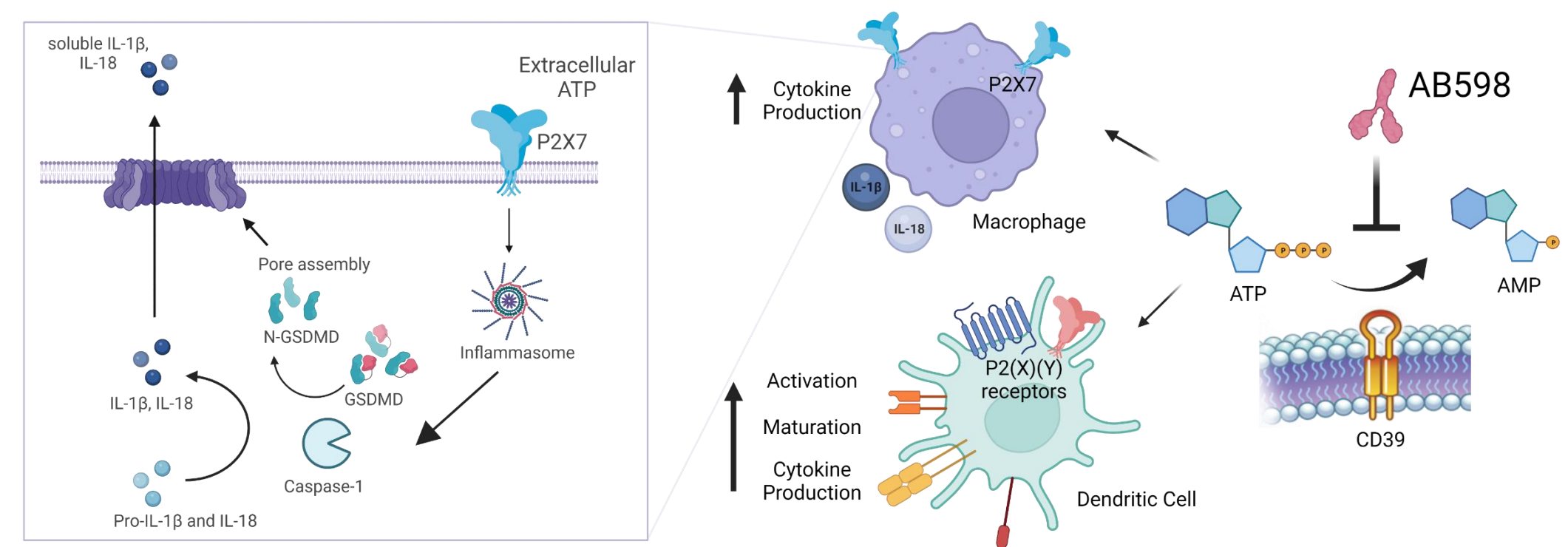


Figure 1. CD39 inhibition promotes anti-tumor immunity by myeloid cell activation. CD39 inhibition by AB598 leads to high levels of extracellular ATP which activates the inflammasome in macrophages and maturation of dendritic cells. Schematic created with BioRender.com.

RESULTS

High CD39 Expression Across Primary Dendritic Cell Subsets and *in vitro*-derived Dendritic Cell and Macrophage Subsets

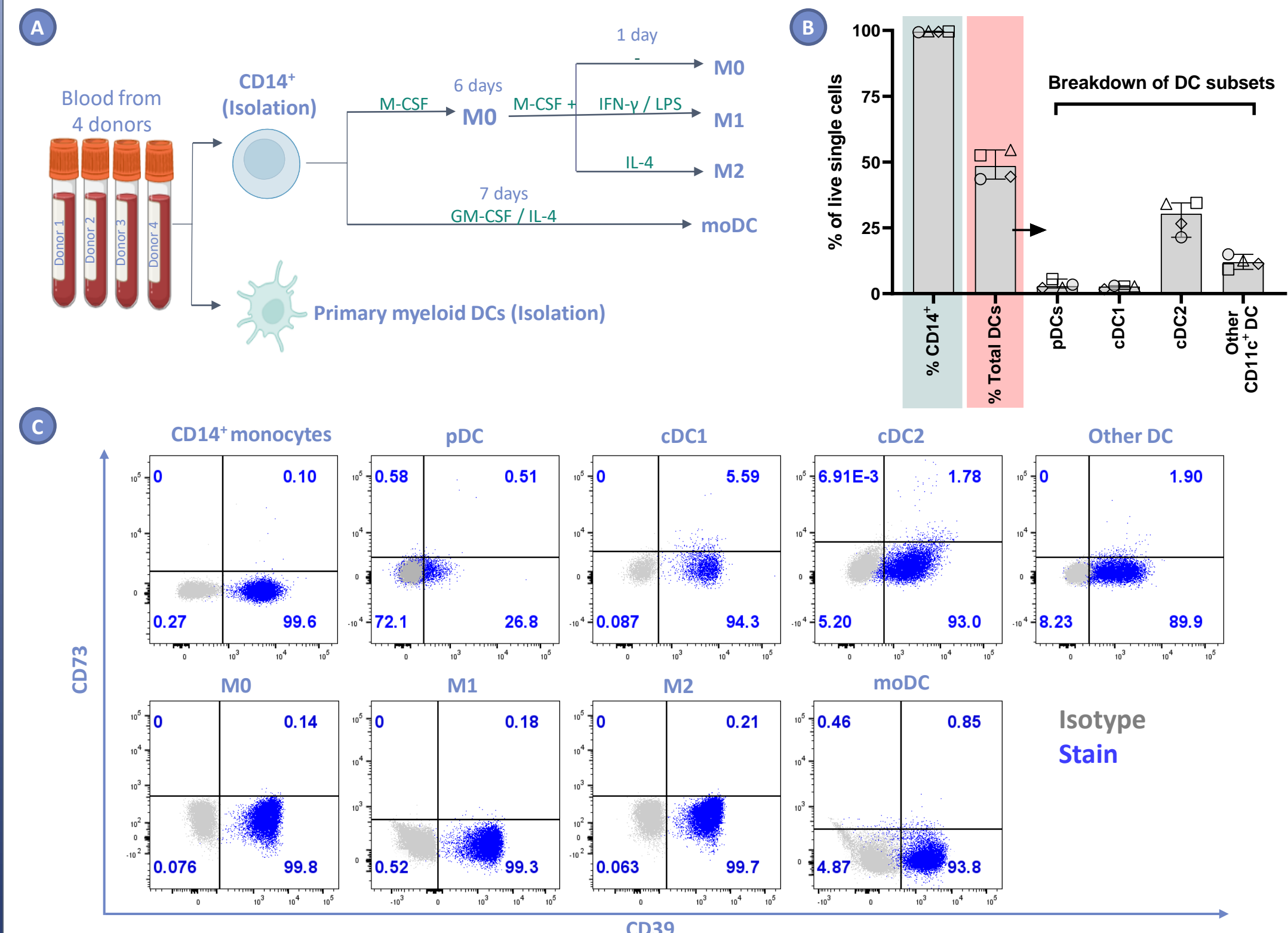


Figure 2. High expression of CD39 across primary and *in vitro*-derived myeloid cell populations. (A) Schematic depicting the isolation and differentiation of the cells used in Figures 2, 3 and 4. (B) The purity of the CD14⁺ monocyte isolation was ~99% and the purity of the myeloid DC enrichment was ~50% total DCs (defined as HLA-DR⁺ CD11c⁺ and pDCs). Also shown is the distribution of DC subsets in the cells resulting from the primary myeloid DC enrichment. (C) Flow cytometry analysis showing the distribution of CD39 and CD73 across myeloid populations from a representative donor. DC subpopulations defined as plasmacytoid DCs (pDCs: HLA-DR⁺ CD11c^{int} CD123⁺), conventional DC1s (cDC1s: HLA-DR⁺ CD11c⁺ CD141⁺ Clec9a⁺), conventional DC2s (cDC2s: HLA-DR⁺ CD11c⁺ CD1c⁺ CD141^{int} Clec9a^{int}) and other DCs (defined as HLA-DR⁺ CD11c⁺ CD1c^{int} CD141^{int} Clec9a^{int}).

In vitro-derived Macrophages Express Highest Levels of CD39

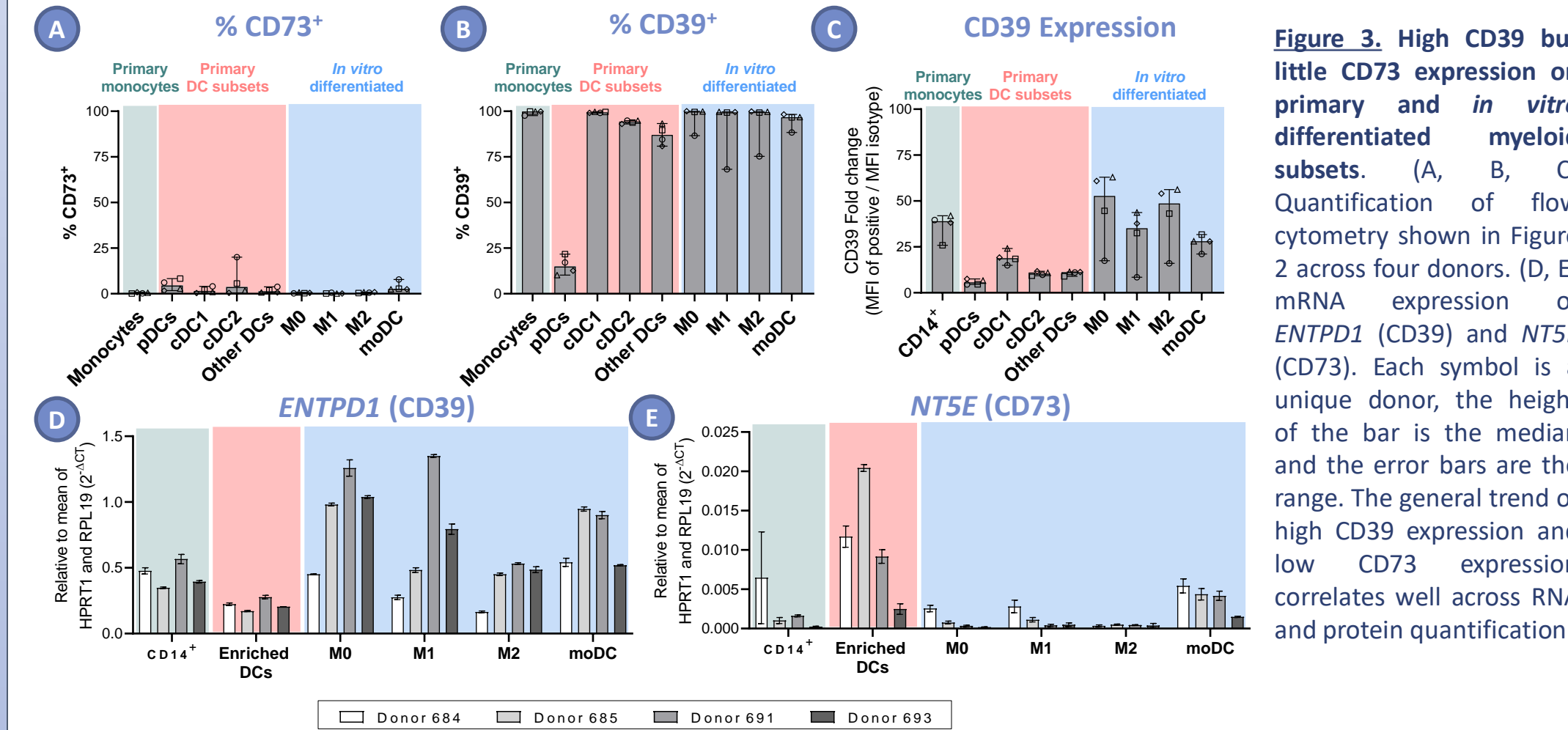
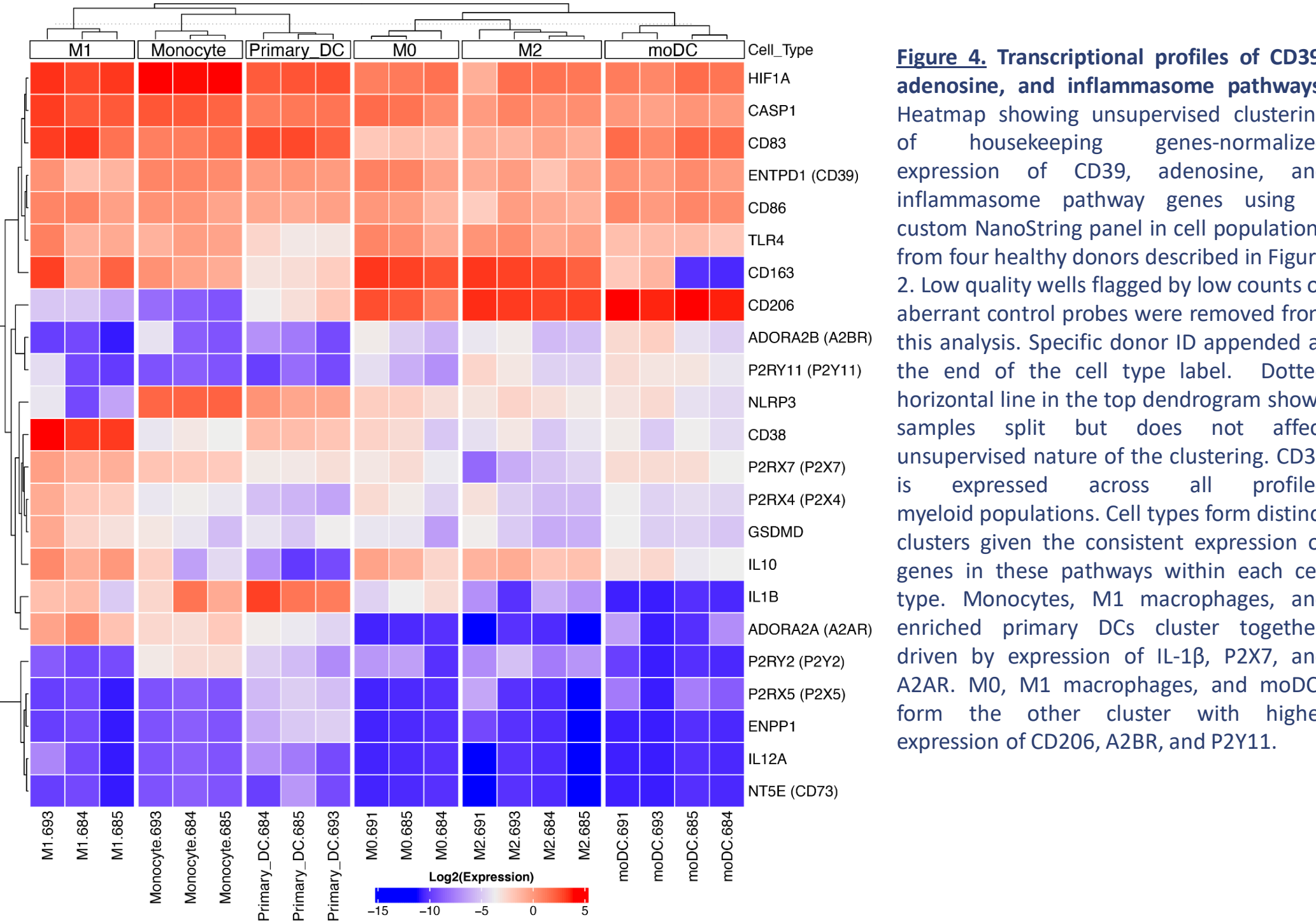


Figure 3. High CD39 but little CD73 expression on primary and *in vitro* differentiated myeloid subsets. (A, B, C) Quantification of flow cytometry shown in Figure 2 across four donors. (D, E) mRNA expression of *ENTPD1* (CD39) and *NT5E* (CD73). Each symbol is a unique donor, the height of the bar is the median and the error bars are the range. The general trend of high CD39 expression and low CD73 expression correlates well across RNA and protein quantification.

Inflammasome-Related Genes are Expressed by All Populations, Highest levels in M1, Monocytes, and Enriched Primary DCs



P2Y11 Antagonism Reduces ATP-Driven Dendritic Cell Activation

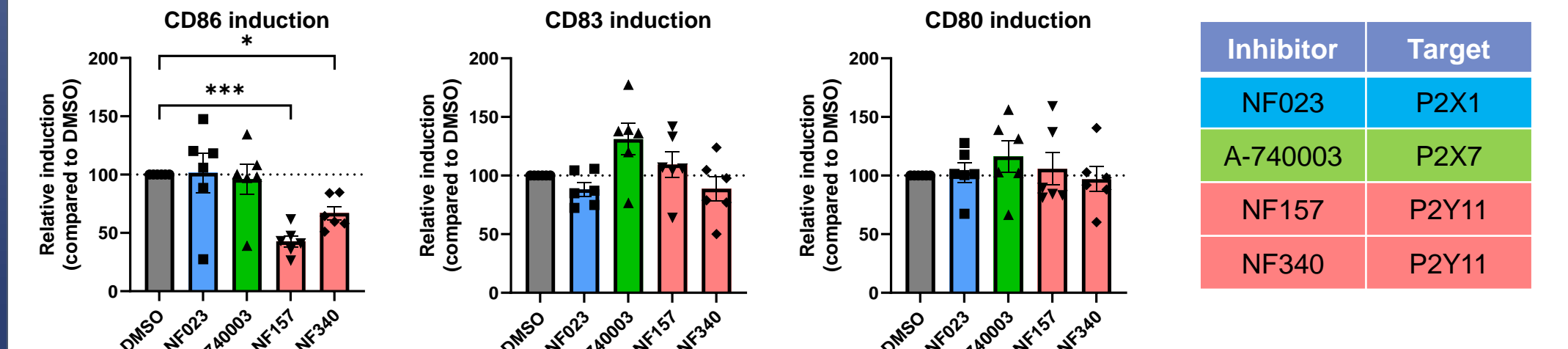


Figure 5. P2Y11 antagonism reduces CD86, a marker of dendritic cell activation. MoDCs were generated by GM-CSF and IL-4 differentiation and treated with 10 μ M of the indicated inhibitor for 1 h followed by 0 or 300 μ M ATP for 18 h. Cell surface marker expression (CD80, CD83, CD86) was assessed by flow cytometry. The induction of activation marker expression from 0 to 300 μ M ATP was compared between inhibitor-treated and DMSO-treated cells. Results show that P2Y11 inhibitors suppress CD86 induction by ATP, but not CD80 or CD83. The height of the bars is the mean and error bars are the SEM. Each symbol represents one donor. Statistical analyses were performed using an ANOVA with Tukey's multiple comparison test, * $p < 0.05$, *** $p < 0.001$.

AB598 Promotes ATP-Dependent Dendritic Cell Maturation and Macrophage Inflammasome Activation

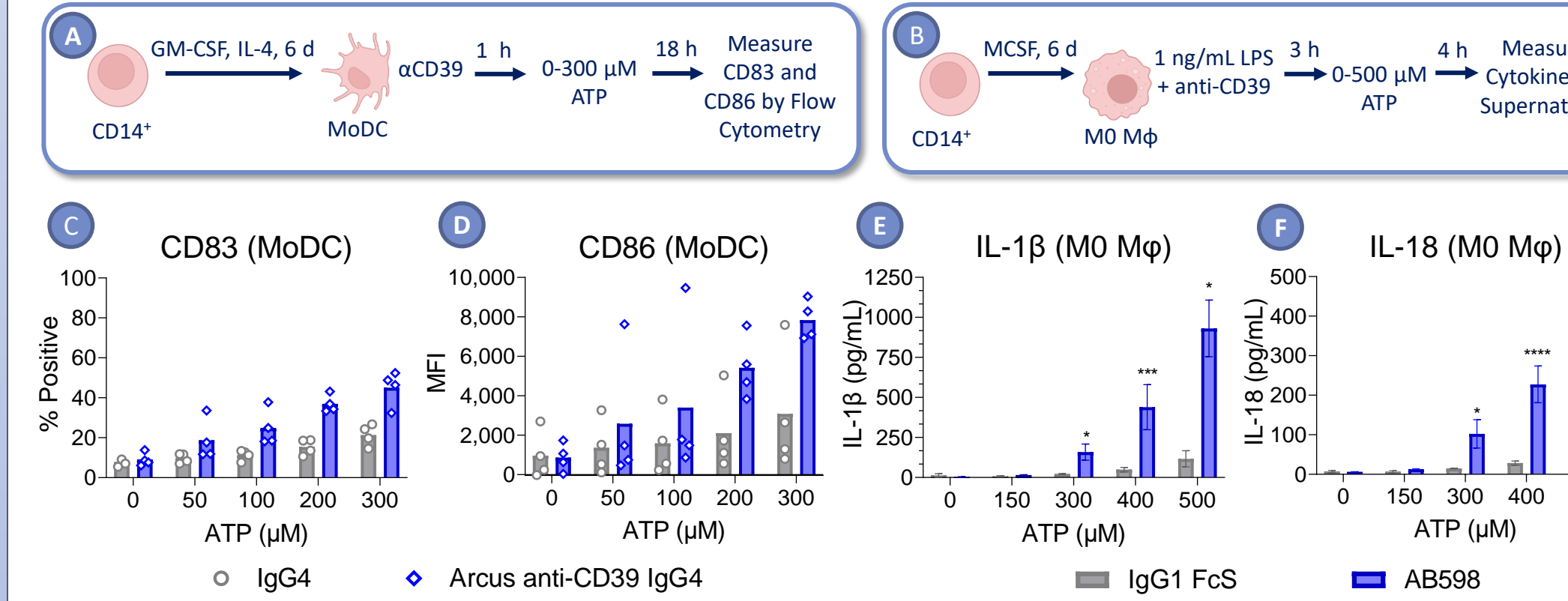


Figure 6. A, C, D. Increased moDC maturation by AB598 treatment in the presence of ATP. CD14 positively selected cells from peripheral blood were differentiated in GM-CSF and IL-4 for 6 days to generate monocyte-derived dendritic cells (moDCs). On day 6, test antibodies were added for 1 hour prior to ATP addition. Post-ATP addition, cells were incubated overnight and subjected to flow cytometry the next day. (C, D) ATP dose response showing an increase in moDC maturation as evidenced by an increase in CD83 and CD86 with increasing amounts of ATP. The effect is amplified by the addition of anti-CD39 antibody. Shown with four donors. **B, E, F. Increased inflammasome activation by AB598 treatment in the presence of ATP.** CD14 positively selected cells from peripheral blood were differentiated in MCSF for 6 days to generate M0 macrophages. Concurrent CD39 inhibition with AB598 and 1 ng/mL LPS stimulation for 3 hours was followed by the addition of ATP for 4 hours. This led to an increase in IL-1 β and IL-18 secretion, indicative of inflammasome activation. Data is shown from three donors and the error bar is the SEM. Statistics were calculated using a ratio paired t-test relative to the ATP-matched isotype control condition where *, $p < 0.05$ and ***, $p < 0.001$. IL-1 β was measured by ELISA and IL-18 by MSD.

Solid Tumors Express the Machinery for Response to Elevated ATP as a Result of CD39 Inhibition

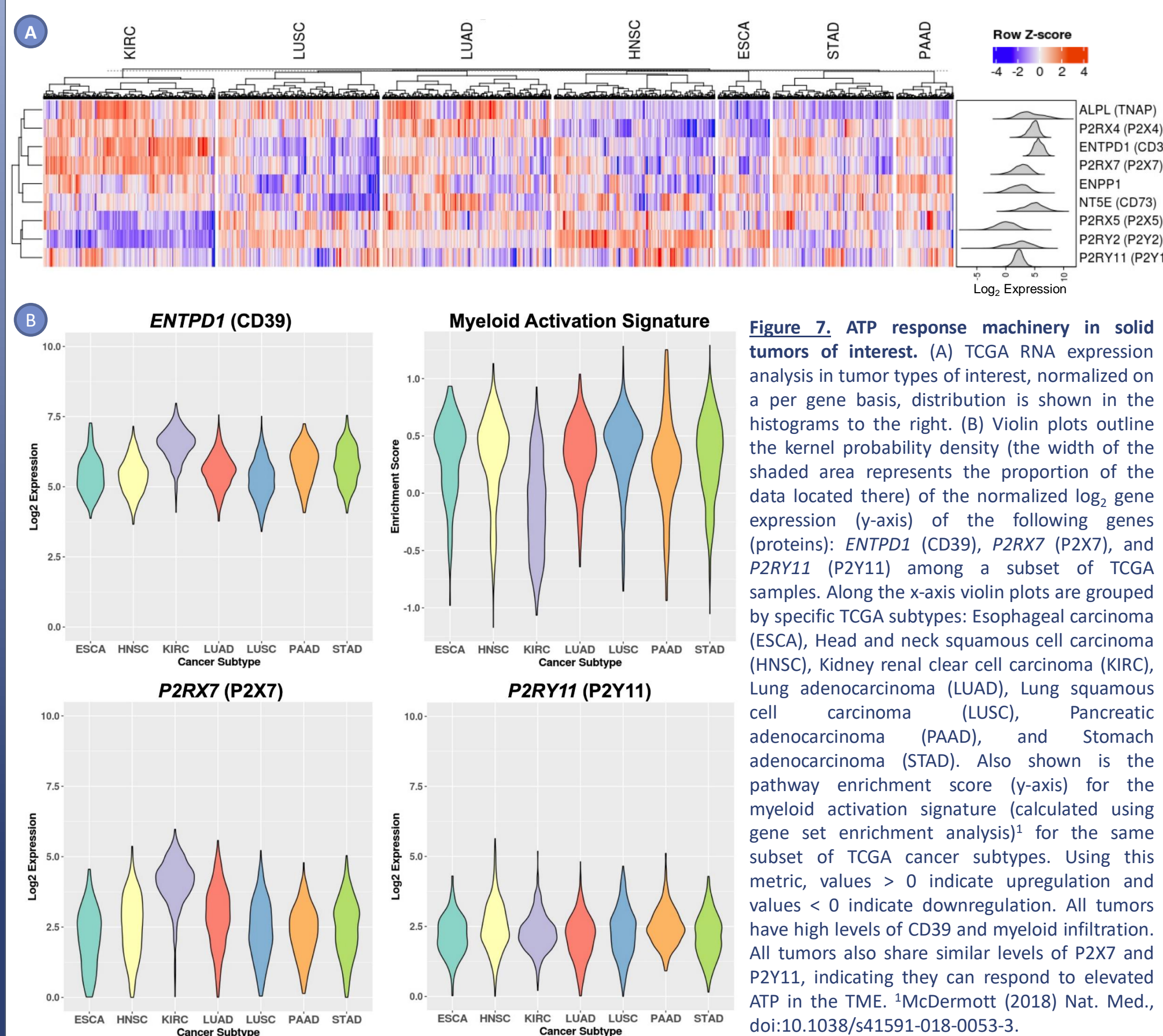


Figure 7. ATP response machinery in solid tumors of interest. (A) TCGA RNA expression analysis in tumor types of interest, normalized on a per gene basis, distribution is shown in the histograms to the right. (B) Violin plots outline the kernel probability density (the width of the shaded area represents the proportion of the data located there) of the normalized log₂ gene expression (y-axis) of the following genes (proteins): *ENTPD1* (CD39), *P2RX7* (P2X7), and *P2RY11* (P2Y11) among a subset of TCGA samples. Along the x-axis violin plots are grouped by specific TCGA subtypes: Esophageal carcinoma (ESCA), Head and neck squamous cell carcinoma (HNSC), Kidney renal clear cell carcinoma (KIRC), Lung adenocarcinoma (LUAD), Lung squamous cell carcinoma (LUSC), Pancreatic adenocarcinoma (PAAD), and Stomach adenocarcinoma (STAD). Also shown is the pathway enrichment score (y-axis) for the myeloid activation signature (calculated using gene set enrichment analysis) for the same subset of TCGA cancer subtypes. Using this metric, values > 0 indicate upregulation and values < 0 indicate downregulation. All tumors have high levels of CD39 and myeloid infiltration. All tumors also share similar levels of P2X7 and P2Y11, indicating they can respond to elevated ATP in the TME. ¹McDermott (2018) Nat. Med., doi:10.1038/s41591-018-0053-3.

Chemotherapy Induces ICD in Melanoma Cell Line AB598 Bolsters Extracellular ATP After Chemotherapy Treatment

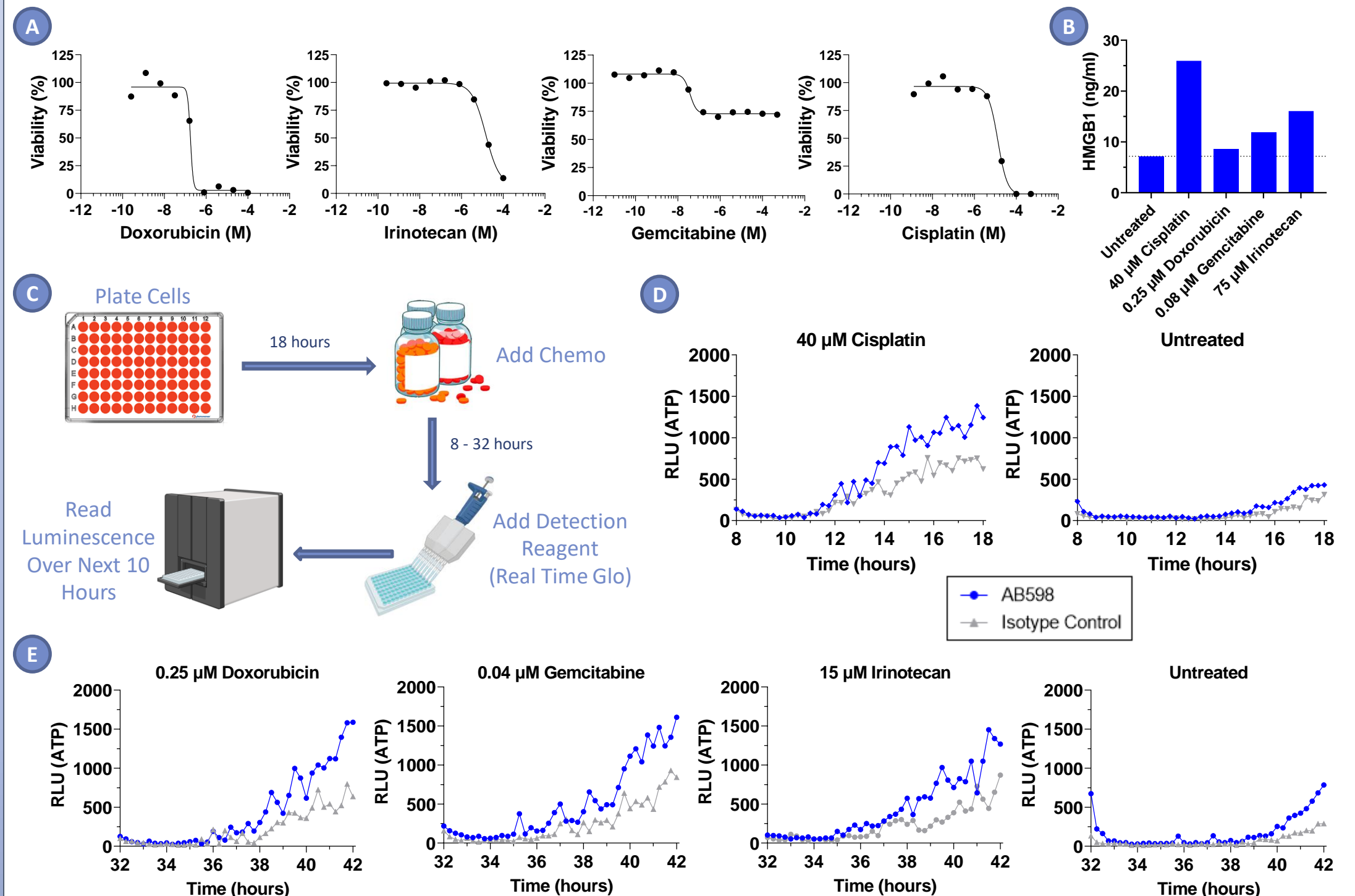


Figure 8. Chemotherapy induces ICD in the human melanoma cancer cell line SK-MEL-5 and AB598 increases extracellular ATP post-chemotherapy treatment. (A) Dose response curves showing the effect of the indicated chemotherapy on SK-MEL-5 viability at 48 h, assessed using Promega CellTiterGlo. (B) HMGB1, a marker of ICD, was measured in the supernatant of SK-MEL-5 cells treated with chemotherapy for 48 h using the Promega Lumit HMGB1 assay. (C) Experimental scheme used to determine chemotherapy-induced extracellular ATP release shown in (D, E). Extracellular ATP in supernatant after 8 - 18 hours (D) or 32 - 42 hours (E) chemotherapy treatment. All chemotherapies tested lead to decreased cell viability and increased ATP release in SK-MEL-5 cells. HMGB1 release is increased with cisplatin, gemcitabine or irinotecan treatment. All chemotherapies tested show hallmarks of ICD, indicating potential for combination treatment with anti-CD39 inhibition in a tumor setting.

CONCLUSIONS

- ❖ CD39 is expressed at both the mRNA and protein level, on both primary and *in vitro*-derived myeloid cell populations.
- ❖ Nanostring profiling confirms CD39 expression and the presence of TLR4, CD83, CD86, and CASP1 across myeloid cell profiles, indicating the presence of necessary components for ATP-induced anti-tumor immunity driven by dendritic cell and inflammasome activation. P2X7 and P2Y11 have complementary expression patterns, which is supported by the finding that P2Y11 antagonism, but not P2X7 antagonism, affects ATP-driven CD86 induction in moDCs.
- ❖ Increases in CD83 and CD86, indicative of moDC maturation, and increases in IL-1 β and IL-18 secretion, indicative of inflammasome activation, are both ATP-dependent, a pattern which is amplified in the presence of the Arcus CD39 inhibitory antibody, AB598.
- ❖ Several solid tumor types express the machinery needed to respond to CD39 inhibition.
- ❖ Several common chemotherapeutic agents are immunogenic cell death (ICD)-inducers and release ATP during cell death. CD39 inhibition by AB598 prevents the degradation of ATP, leading to higher extracellular concentrations of immunostimulatory ATP.
- ❖ **Taken together, AB598 can amplify the effects of ICD-inducing chemotherapy to enhance myeloid cell activation, boosting anti-tumor immunity in solid tumors.**

CONTACT

Kaustubh Parashar, PhD (kparashar@arcusbio.com)
Christine Bowman, PhD (cbowman@arcusbio.com)